Digital correction of computed X-radiographs for coral densitometry

Nicolas Duprey, Hugues Boucher, Carlos Jiménez

Digital correction of computed x-radiographs for coral densitometry

Duprey Nicolas[1*], Boucher Hugues[1], Jiménez Carlos[2, 3]

[1] IPSL / LOCEAN, UPMC / CNRS / IRD / MNHN, IRD Bondy, 93143, France.

[2] Centro de Investigación en Ciencias del Mar y Limnología (CIMAR), Universidad de Costa Rica, San Pedro, 11501-2060 San José, Costa Rica.

[3] Present address: Energy, Environment and Water Research Center (EEWRC) of The Cyprus Institute. P.O. Box 27456, CY-1645 Nicosia, Cyprus

*Corresponding author:

nicolas.duprey@ird.fr

Institut de Recherche pour le Développement IRD

32 Avenue Henri Varagnat

93140 Bondy France

Telephone: +33-688932745

Fax: +33-148025554

Abstract

The recent increase in sea surface temperature and ocean acidification raises major concerns about the evolution of the coral calcification rate. Digitized x-radiographs have been used for coral skeleton density measurements since the 1980s. The main limitation of coral densitometry from digitized x-radiographs is the x-ray intensity heterogeneity due to spherical spreading (inverse square law) and heel effect. Until now, extra x-ray images or aluminum standards have been used to correct x-radiographs. However, such corrective methods may be constraining when working with a high number of coral samples. Here, we present an inexpensive, straightforward, and accurate Digital Detrending (DD) method to correct the heterogeneities of the x-ray irradiation that affect x-ray images. The x-radiograph is corrected against the irradiation imprint recorded by its own background using a Kriging interpolation method, thus allowing reliable optical density measurements directly on the corrected x-ray image. This Digital Detrending (DD) method was validated using skeletal bulk density measurements and Computerized Tomography (CT). Coral densitometry using DD corrected x-radiographs does not require the destruction of the coral sample and provides high-resolution measurements. Since DD does not require extra aluminum standards to correct x-radiographs, this method optimizes the working space available on the x-ray image. Moreover, it corrects the entire x-radiograph, thus larger samples or numerous samples can be x-rayed at the same time.

Keywords: Coral densitometry, calcification rate, density, coral skeleton, Siderastrea siderea, Porites sp.

Introduction

Recent changes evidenced in global Sea Surface Temperature (SST) and oceans' pH, raise major concerns about the future of coral reefs (Kleypas, 1999; IPCC, 2007, 2007; Pandolfi et al., 2011). A major consequence of ocean pH decrease is the diminution of the aragonite saturation state (Ω_{arag}). A compilation of data documenting calcification response to the Ω_{arag} decrease among individual coral species, coral mesocosms and in situ reef communities, showed that this response was consistently negative (Pandolfi et al., 2011). Since the early 1990's an unprecedented declining trend of the coral calcification rate (product of the annual extension rate and the coral skeleton density) has been observed in Great Barrier Reef records, most probably due to the recent increase in SST and to ocean acidification (Cooper et al., 2008; De'ath et al., 2009). Conversely, coral response to combined ocean warming and pH decrease appears highly variable and often non-linear. Moreover, coral response is also greatly influenced by other factors such as nutrients, pollutants or salinity so that projecting the future of coral reefs in a global warming and ocean acidification context is still uncertain (Pandolfi et al., 2011). As stated by the IPCC report (2007) "acidification is an emerging issue with potential for major impacts in coastal areas, but there is little understanding of the details. It is an urgent topic for further research, especially programmes of observation and measurement". Documenting the long term trends in coral calcification is crucial in understanding the mechanisms and implications of ocean acidification on coral reefs, in order to predict coral reef future.

Coral calcification rate (CR) is calculated by **CR = ER x d**, where (**ER)** is the annual extension rate and (**d)** is the coral skeleton density. Whereas extension rate can be directly measured from the banding pattern revealed by x-radiography, many methods have been developed since the 1970s to measure skeletal density. Direct measurements have been performed based on mercury displacement (Dustan, 1975), water displacement (Hughes, 1987) and coral pore volume calculation (Carricart-Ganivet et al., 2000). Although these methods provide reliable measurements, they are time consuming, imply the destruction of the sample and provide low measurement resolution (generally performed by sampling annual growth increments). Methods that do not require the destruction of the coral sample, such as gamma densitometry (Chalker and Barnes, 1990) or medical x-ray Computerized Tomography (CT) (Bosscher, 1993) are quick and provide higher resolutions (less than one millimeter, i.e., monthly resolution or higher). However, these methods rely on specialized and expensive equipment, not always easily accessible. Alternative methods for coral skeleton density measurement are based on digitized x-radiographs (Chalker et al., 1985; Helmle et al., 2000; Carricart-Ganivet and Barnes, 2007). Optical densities (OD)[1] of x-radiographs are measured on film or on digital images and converted into density values using OD reference standards (e.g., Tridacna maxima shells and/or aluminum wedges).

An important drawback is that x-radiographic instruments do not provide uniform irradiation of the entire area covered by the x-ray film and may therefore result in misleading density measurements. Two reasons account for such irradiation heterogeneities: the heel effect which is defined by an irradiation gradient along the anode-cathode axis and the inverse square law which states that the irradiation is inversely proportional to the square of the distance from the x-ray source (Meredith and Massey, 1971; Chalker et al., 1985; Helmle et al., 2000; Carricart-Ganivet and Barnes, 2007). The irradiation gradient caused by the heel effect may lead to biases in density measurements up to 26% (Chalker et al., 1985), which is similar to the seasonal density variations that are reported for massive corals Montastrea annularis (20% - Carricart-Ganivet and Barnes, 2007), Porites sp. (15% - this study) and Siderastrea siderea

1 In the following study the Optical Density (OD) refers to the grey level from 0 to 255 corresponding to the 8 bits coding of the digital images.

(30% - this study). Several alternative methods have been proposed to overcome such miscalculations. For example, Helmle et al. (2002) performed paired x-radiographs (using the same settings) of a coral sample and an aluminum plate. Therefore, it was possible to correct the coral sample image from the irradiation heterogeneities recorded by the aluminum plate's x-radiograph. However, considering that each x-radiograph has to be taken twice, this technique becomes expensive and time-consuming when a high number of samples have to be analyzed. Carricart-Ganivet and Barnes (2007) proposed a simple way for correcting the heel effect. The correction is based on the measurement of OD variations on an aluminum bar located beside the coral sample along the anode-cathode axis. The heel effect-related distortions are then measured, and extrapolated over coral samples. The method provides a reliable one-dimensional correction along the anode-cathode axis. Unfortunately, the extrapolation of this correction to the whole x-radiograph image may only be applied upon particular settings (x-ray source to film distance and film dimension).

In the present study, we introduce a Digital Detrending (DD) method which corrects the heterogeneously irradiated x-radiographs. This method is inexpensive, straightforward and accurate. The DD method uses the x-ray irradiation imprint, recorded by the x-radiograph's background, to reconstruct a full image of the irradiation pattern. The x-radiograph's background is defined here as the image area without any objects or graphical information such as letters or numbers. The resulting modeled image is then subtracted from the original x-ray image, therefore enabling reliable optical density measurements from the corrected x-ray image. This method provides a correction of x-ray irradiation heterogeneities on the whole x-radiograph, which means a two-dimensional correction. The Digital Detrending (DD) method was used for densitometry measurements on samples of widely studied massive corals Porites sp. and S. siderea (Guzman and Tudhope, 1998; De'ath et al., 2009; Lough and Cooper, 2011).

Materials and Methods

Computed x-radiography

Experiments were performed using a medical Computed Radiography (CR) device. CR produces digitized images obtained directly from an imaging plate (IP) instead of a conventional photo sensitive film. IP is placed beneath coral slabs before being irradiated (Fig. 1a). The final result is an 8 bits digitized image (pixel values comprised between 0 and 255). Such an image can be used for Optical Density (OD) measurements and be easily modified with conventional image-processing software. CR is affected by heterogeneous x-ray irradiation just like conventional radiography.

The CR device was a SUPER CONTACT® x-ray device (General Electric Company). X-radiographs were acquired with FUJI® imaging plates made of photosensitive phosphorus. Digitized images were then obtained using an IP reader (FUJI® FCR 5000). The resolution of this device is lower than conventional x-radiography.

X-ray irradiation heterogeneities

Heel effect - The heel effect is responsible for the irradiation intensity gradient along the anode-cathode axis: the electrons emitted from the cathode interact with the anode resulting in a high exposure at the cathode side of the IP and a decrease toward the anode side (Fig. 1b).

Inverse square law - The inverse square law models the three-dimensional spherical spreading of the x-ray beam: irradiation intensity is attenuated by a factor proportional to the inverse of the squared distance from the x-ray source to the IP surface. As IP are generally centered beneath the x-ray source, the irradiation pattern shows over-exposed area at the center of the image, decreasing toward the edges (Fig. 1b). The influence of spherical spreading on the irradiation pattern gets lower with increasing source-subject distance.

The inverse square law specifies that the ratio of x-ray intensity on the IP (I_1) to intensity on the subject surface (I_2) is:

$$\frac{I_1}{I_2} = \frac{(S_p - s)^2}{(S_p)^2} \quad (1)$$

Where Sp = source to IP distance and s= sample thickness.

Computed Tomography

Computed Tomography (CT), with its high-contrast resolution, allows accurate and reliable density measurements, as this method is not influenced by the x-ray beam distortion phenomena that usually affect computed radiography. A CT-scan was used to compare density profiles measured on DD corrected images to the density profile of the CT scan. The Computerized Tomography device used was a Phillips Brilliance 40®. CT density values are expressed as Hounsfield units.

Reference materials

We used two massive corals slabs as reference samples. Reference slab R_s was cut off a core drilled in 2008 from a living colony of the reef-building species S. siderea at Cahuita reef (9°44’N - 82°48’W), Limón, Costa Rica. R_s size was 280 x 70 mm; slab thickness (s) was 5 mm. Reference slab R_p was cut off from a living colony of the reef-building species Porites sp. at the Fausse Passe de Uitoé reef (22°17'S - 166°10'E), New-Caledonia, France, in 2010. This coral was collected alive and transferred into an aquarium in 2008. R_p size was 150 x 150 mm and the slab thickness (s) was 10 mm. For coral density measurements, a reference transect for both slabs was set along the maximum growth axis, perpendicular to the growth increments. For R_s, the reference transect tr_S was 87 mm long and encompassed 15 couplets of high and low density bands; for R_p, the reference transect tr_p was 130 mm long and encompassed 13 couplets of high and low density bands. In order to avoid as much as possible intra-corallite density variations, the width of the density transects was 10 mm to include approximately three S. siderea corallites (polyps mean diameter ~ 3 mm) and ten Porites sp. corallites (polyps mean diameter ~ 1 mm).

Density scaling

Density scaling is based on two, two-sided wedges (d_{clam} – Fig. 1c) cut from the internal layer of a giant clam's shell Tridacna squamosa. One wedge is 17.4 mm high and 54.2 mm long with slopes of 26.6° and 41.2°. The second wedge is 15.9 mm high and 71.8 mm long with slopes of 43.4° and 16.0°. The bulk densities of the wedges were obtained by weighting with a hydrostatic balance.

Care should be given when cutting a wedge into a giant clams' shell as it is composed of three distinct aragonitic layers (internal layer, external layer and hinge layer) which present their distinct density and crystallographic structure (N. Duprey, unpublished data). To avoid any measurement bias, wedges must be cut into either external or internal shell layer. X-radiographs revealed that the density of the whole shell's internal layer (d_{shell}) was homogeneous.

To ensure the consistency of the density scaling, another scaling standard (d_{powder}) was added on some x-radiographs for comparison purposes. Standard d_{powder} is composed of 14 plastic cubes filled with Porites sp. coral aragonite powder (grain size < 200 µm). Each cube was filled with a carefully weighted amount of powder to obtain a density scale from 0 to 3 for an equivalent sample thickness of 12 mm.

Both plastic cubes filled with coral powder and wedges have a similar range of density values. However, wedges were favored for their small sizes because this optimizes the space available on the x-radiograph, so that more coral samples can be x-rayed at the same time.

X-radiographs

All the x-radiographs and their characteristics are listed in table 1. For this study, we used eight x-radiographs made with the CR device previously described. The main purpose of these x-radiographs was to test the reliability of the Digital Detrending method depending on the distance Sp and samples orientation along the anode-cathode axis. Therefore, coral reference samples were placed along three directions with regard to the anode-cathode axis: perpendicular, parallel and diagonally. Selected distances (Sp) were 130cm, 100cm and 80cm. X-radiographs were acquired over a two-year period, providing the opportunity to test the DD method against a potential machine drift over time.

Merely considering the inverse square law and the IP size (355 x 428 mm), the minimum exposures at image edges would be 11.8%, 8.1% and 5.0% less than the exposures at the center for Sp=80cm, Sp=100cm and Sp=130cm, respectively.

X-radiograph C2 was used to test the density calibration of the two density standards (d_{powder} and d_{clam}). For that purpose we used 13 Porites sp. cubes (~ 2cm^3) which bulk densities were determined by weighting with a hydrostatic balance. Coral cubes density ranged from 1.21 to 1.39 $g.cm^{-3}$.

Digital Detrending procedure

The first stage of the digital detrending (DD) process is the background area selection. This area is used as a recorder of the irradiation pattern. The background area selection aims to remove all saturated margins, all pixels corresponding to samples and optical density scale or information, from the original x-radiograph (Fig. 2a). This background extraction is made using the magic stick tool of the image processing software GIMP® (or equivalent). This step leaves empty areas corresponding to objects' locations (Fig. 2b). Missing OD values are interpolated using a Kriging interpolation from the dacefit MATLAB® toolbox (Lophaven et al., 2002). The result is a complete image of OD variations (Fig. 2c) following the overall pattern presented by the original background area. The corrected image is obtained by subtracting the modeled background to the original image (Fig. 2d).

The DD method initially supposes that the x-ray intensity at the IP surface is similar to the x-ray intensity at the sample surface. However, x-ray source to sample surface distance (Ss) is smaller than x-ray source to IP surface distance (Sp). Considering equation (1), it can be stated that the spherical spreading causes the x-ray intensity to be higher at the sample surface than at the IP surface. This may generate a small bias in measurement, thereafter referred as thickness bias, leading to a slightly overestimated density. This bias can be reduced by decreasing the sample thickness and corrected during the DD process by dividing corresponding background values with the ratio I_1 / I_2.

X-ray attenuation in air may also account for the difference between x-ray intensities at sample and IP surfaces. Coral densitometry studies are usually performed on samples with thickness less than 10 mm. According to the air mass attenuation coefficient table from the National Institute of Standards and Technology, x-ray attenuation for a 10 mm air layer is negligible (Table 2).

Digital Detrending evaluation

In order to optimize the DD procedure we had to test first if the x-ray irradiation imprint on the IP remains identical while maintaining the x-ray source settings and the Sp distance constant (α). If this last assumption is true, then a standard correction could be used within a group of x-radiographs made with the same settings. Therefore, the DD procedure would be simplified and faster. If not, each x-radiograph should be corrected with the irradiation record of its own background. By taking pair-wise images, α was tested using the mean relative difference of OD ($\Delta OD_{(i,j)}$).

The relative difference of OD ($\delta OD_{(i,j,k)}$) at point k for images i and j is defined as:

$$\delta OD_{i,j,k} = \frac{\left| (OD_i(x_{(k)} y_{(k)}) - OD_j(x_{(k)} y_{(k)}) \right|}{OD_i(x_{(k)} y_{(k)})} \quad (2)$$

Where OD_i ($x_{(k)}$,$y_{(k)}$) is the OD value at image coordinates ($x_{(k)}$,$y_{(k)}$) for image i and OD_j ($x_{(k)}$,$y_{(k)}$) is the OD value at image coordinates ($x_{(k)}$,$y_{(k)}$) for image j.

The mean relative difference of OD ($\Delta OD_{(i,j)}$) for images i and j is:

$$\Delta OD_{i,j} = \frac{1}{n} \cdot \sum_{k=1}^{n} \delta OD_{i,j,k} \quad (3)$$

Where n is the number of pixels coordinates shared by images i and j backgrounds.

Considering the causes of the x-ray irradiation heterogeneities, the reliability of the Digital Detrending process had to be tested through two other assumptions.

The DD method corrects and preserves the density information of the sample independently of:

(β) - the sample orientation along the anode-cathode axis

(γ) - the distance S_p

The density information of the coral samples refers to the density variability (qualitative information) and to the density value (quantitative information). β was tested by measuring the coral density profiles (tr_S and tr_p) on samples set perpendicularly, parallel and diagonally to the anode/cathode axis, while the other settings remained unchanged. Intra-group A density transects comparisons evaluated the ability of the DD method to correct the irradiation heterogeneities mainly caused by the heel effect (independently of the samples orientation along the anode-cathode axis). Intra-group B density transects comparisons evaluated the correction of both the heel effect and the inverse square law heterogeneities (independently of the samples orientation along the anode-cathode axis). γ was tested by inter-groups (A and B) comparisons. The comparison of inter-groups (A, B and C) was used to assess the ability of the DD method to cope with a potential machine drift over time. Finally, to ensure that the DD method yields the same density variations as other density measurement techniques, the density measurements made on a DD corrected image were compared to Computed Tomography scanning measurements.

To test the previous assumptions, density values were measured along tr_S and tr_p for each x-radiograph. The correlation between the density profiles was tested using the regression coefficient R^2. Furthermore, relative standard deviations (rsd) were calculated at each point along transects of the compared x-radiographs and averaged in order to compile the results. These mean Relative Standard Deviation (RSD) values were used to evaluate the precision (reproducibility) of density measurements.

The mean Relative Standard Deviation (RSD) for compared transects is defined as:

$$RSD = \frac{1}{p} \cdot \sum_{i=1}^{p} rsd_i \quad (4)$$

Where p is the number of points along the compared transects [$p(tr_s)$=439 and $p(tr_p)$=666] and rsd_i represents the relative standard deviation of the density at point i.

Density calibration

OD values were converted into densities using the two, two-sided wedges cut from the internal layer of a giant clam's shell Tridacna squamosa. The OD values on DD corrected x-radiographs were measured along the two sides of both wedges using the ImageJ® software. As giant clam shell also contains organic matter, which influences bulk density, wedges thicknesses had to be corrected in order to obtain equivalent thicknesses, corresponding to wedges made of pure aragonite. Thereafter, a wedge's equivalent thickness was defined as T_{W100}.

The equivalent thickness scaling at each point along a wedge was calculated by:

$$T_{w100} = \frac{T_x \cdot d_{shell}}{d_{arag}} \quad (5)$$

Where T_x = measures wedge thickness, d_{shell} = shell wedge density (g.cm^{-3}) and $d_{arag.}$ = density of pure aragonite (2.930 g.cm^{-3}).

OD values were then paired with corresponding equivalent thicknesses (T_{W100}) calculated along the wedges. Paired OD and T_{W100} values from the two wedges were pooled and fitted by a quadratic polynomial function:

$$OD = a \cdot T_{w100}^{2} + b \cdot T_{w100} + c \quad (6)$$

Where a, b and c constants are the coefficients determined by the polynomial fitting for the studied x-radiograph.

Equation (6) obtained from the wedges' data was then reversely used to convert OD values of coral samples into pure aragonite equivalent thicknesses (T_{S100}). Subsequently, coral sample density values (d) were obtained from T_{S100}:

$$d = \frac{T_{s100}}{T_s} \cdot d_{arag} \quad (7)$$

Where d = coral sample density ($g.cm^{-3}$), T_{S100} = pure aragonite equivalent thickness for coral sample, T_s = measured coral sample thickness; d_{arag} = density of pure aragonite (2.930 $g.cm^{-3}$).

Calibration's validation

In order to validate our density calibration using T. squamosa wedges, OD measurements were performed on coral cubes and plastic cubes filled with coral powder on the detrended x-radiograph C1. OD values were converted into densities using previous equations (5) to (7). These values were regressed against bulk density measurements performed on the same coral and plastic cubes standards.

The relative error (re_i) of x-radiograph density measurements was calculated for each coral cube:

$$re_i = 100 \cdot \frac{| d_{calc.(i)} - d_{bulk(i)} |}{d_{bulk(i)}} \quad (8)$$

Where $d_{calc.(i)}$ is the density of coral cube i calculated from OD after digital detrending ($g.cm^{-3}$) and $d_{bulk.(i)}$ is the bulk density ($g.cm^{-3}$) of coral cube i.

The mean Relative Error (RE) of x-radiograph density measurements was evaluated by averaging the relative errors (re_i) of coral cubes:

$$RE = \frac{1}{n} \cdot \sum_{i=1}^{n} re_i \quad (9)$$

Where n=14 is the number of coral cubes (Porites sp.).

RESULTS

Reproducibility of the irradiation imprint (α)

The background area of the eight x-radiographs viewed in false colors show a strong OD gradient along the anode-cathode axis, with low OD at the anode side increasing toward the cathode side. This pattern is characteristic of the heel effect (Fig. 1a). A concentric OD pattern, characteristic of the spherical spreading, is noticeable on some images. As expected, x-radiographs with high distance Sp (groups A) present a less marked concentric pattern than x-radiographs with low distance Sp (group B). OD mean relative difference (ΔOD) of x-radiographs backgrounds ranges from 8% up to 290% (Table 3). Intra-group and inter-group comparison lead to similar ΔOD: most x-radiographs present highly variable background OD values: assumption α is thus not valid within our experimental settings.

Influence of the sample orientation along the anode-cathode axis (β) and of the Sp distance (γ)

Density profiles measured on corrected x-radiographs of groups A and B are well correlated (Table 4). Inter-group and intra-group correlation coefficients values (R^2) are significant and have a similar range from 0.90 to 1.00 ($p<0.001$).

Inter-group and intra-group mean relative standard deviation (RSD) of densities measured on uncorrected images range from 10.1 to 16.0% (Table 5). Density profiles measured on corrected images show a RSD reduced by a factor of 2 to 3. No differences are noticed between the inter-group RSD and intra-group RSD, which are both around 4-5%.

The variations and the precision of density measurements from the corrected images show no difference regarding the sample orientation along the anode-cathode axis (β) or the Sp distance (γ). Assumptions β and γ are thus validated within our experimental settings.

Density measurement precision on DD corrected images

RSD calculated over all uncorrected x-radiographs (groups A, B and C, 14 transects= 7 x tr_s and 7 x tr_p) reaches 16.1% (Table 5). RSD calculated over all DD corrected x-radiographs is 6.8%. These values include measurements made on x-radiographs of two coral samples of different genus, set on three different ways along the anode-cathode axis, with three different distances (Sp), made across a two-year period.

Density variations

The tr_s and tr_p density profiles, measured on uncorrected images, shown as examples on figure 3, present seasonal density variations comprised around 30 and 15% respectively. Profile tr_s

measured on the uncorrected image presents an increasing trend with a maximum density difference reaching 50%. The mean profile tr_s from DD corrected images does not present any remarkable trend. This mean profile tr_s shows density variations identical to the CT scan density profile variations (Fig. 3a). This correlation is a robust result as each of the seven density profiles tr_s, measured on corrected x-radiographs, are significantly correlated with the density profile made on the CT scan ($0.89 < R^2 < 0.96$; $p<0.001$; Table 6). The DD method thus eliminates the density trend caused by the x-ray heterogeneities. Conversely, the magnitude of the seasonal density variations is not affected by the DD correction.

Profile tr_p from the uncorrected image (Fig. 3b) displays a density drop that matches with the transfer of sample R_p from the reef to the aquarium. This profile also displays a parabolic trend with a maximum density difference reaching 50%. The DD method removes the parabolic trend of the profile tr_p, and highlights a linear declining trend with density difference reaching 40%. The density drop (sample R_p transfer) is not affected by the DD correction.

Density Calibration

The four sides of the two, two-sided T. squamosa wedges (Fig. 1c) returned identical OD versus T_{w100} profiles (R^2=0.9998, $p<0.001$, Fig. 4). Density values, calculated from corrected x-radiograph C2, are regressed against the bulk density values (coral cubes and plastic cubes filled with coral powder – Fig. 5). This regression presents a significant correlation coefficient (R^2=0.99; $p<0.001$; n=27). Comparison between bulk densities of the 14 Porites sp. coral cubes and the calculated density values show that the mean relative error (RE – equation 9) is 3.32%.

DISCUSSION

Computed x-radiographs commonly show an uneven exposure due to both the heel effect and the spherical spreading. Such irradiation heterogeneities may lead to variations in coral density up to 50% (Fig. 3). These density variations exceed the seasonal variations commonly observed in massive coral: 30% for Siderastrea siderea, 15% for Porites sp. and about 20% for Montastrea annularis (Carricart-Ganivet and Barnes, 2007). These variations in density may lead to biased calcification rate calculation and thus to wrong environmental interpretations.

The Digital Detrending method, presented here, aimed to correct the irradiation heterogeneities that affect conventional and computed x-radiography. X-radiographs were corrected against the irradiation pattern recorded by the background of the image. The first step of this study was to test if the x-ray irradiation imprint on the Imaging Plates (IP) remains identical while maintaining the x-ray source settings and the Sp distance constant. Our results showed that the x-ray irradiation imprint recorded by the IP was highly variable, even within constant x-ray source settings and Sp distance. X-ray irradiation records must be considered as unique and thus cannot be transposed to another x-radiograph, even within constant settings. These results are in accordance with previous studies (Chalker et al., 1985; Carricart-Ganivet and Barnes, 2007). The x-ray irradiation records may be affected by several factors including the x-ray device stability, the x-ray tube aging and also the recording abilities of the IP or film sensitiveness (Carricart-Ganivet and Barnes, 2007).

Density profiles from DD corrected x-radiographs were highly correlated to the density profile measured on the Computed Tomography scan. These R^2 correlation values were not affected by the orientation of the sample along the anode-cathode axis and the distance from the x-ray source (Table 6). The DD method was thus able to correct x-radiographs of coral samples, showing strong irradiation heterogeneities; independently of the sample orientation along the anode-cathode axis and the distance from the x-ray source. Furthermore, this study revealed that the coral intrinsic density variations (e.g., seasonal density variations or punctual events) contained by the x-radiograph are preserved during the DD process (Fig. 3).

The mean relative error on density measurements of 14 coral cubes of Porites sp., using giant clam Tridacna squamosa wedges as density standard (equation 9), was 3.32%. Causes of such an error may be related to the IP sensitiveness (i.e., signal to noise ratio) and to the chemical composition differences between giant clams shell and coral skeleton that could induce a bias up to two percent in density measurements (Chalker et al., 1985). Carbonate structure differences between coral slabs and shell wedges may also contribute to this error, potentially generating diffusion and/or diffraction of the incident x-ray**.**

Enhancing the number of density measurements from 14 up to 7735 measured points (439x7 tr_s values and 666x7 tr_p values), the overall precision of the coral densitometry from DD corrected x-radiographs reaches 6.8% (Table 5 and Fig. 3). It is important to notice that this value includes the error intrinsic to x-radiography device (noise of the recorded x-ray signal and potential machine drift over time), the error related to the DD correction itself and the error of the density calibration process. This value is noteworthy compared to the biases in density measurements, caused by uncorrected irradiation heterogeneities that reach up to 50%. In addition, the overall error on density measurement is below the range of the seasonal density variations reported previously for massive coral skeleton.

The efficiency of our DD method relies on the x-ray irradiation pattern recorded by the background. As a result, it is necessary to optimize the background area all over the x-radiograph: samples must be scattered all over the IP with spacing of a few centimeters in between and from the plate edges. We recommend to space x-rayed objects by more than one centimeter between each and to keep a two centimeter margin from the edges. Consequently, larger samples or numerous samples can be x-rayed at the same time and compared on the same image as shown on x-radiograph C1 (Fig. 2). The DD method is straightforward, as it does not rely on specific radiography device settings and does not need any prior assumption on the causes of x-ray beam heterogeneities. DD method saves time as it does not require extra x-radiographs to correct the irradiation heterogeneities. Our detrending method could also be applied onto digitized conventional x-radiographs. The DD method applied to such x-radiographs would provide the opportunity to perform qualitative density measurements on x-radiographs from previous studies. Quantitative density measurements would be even possible for x-radiographs acquired with a density scale.

The Digital Detrending method is a powerful tool for monitoring the impact of ocean acidification and global warming on coral calcification rates. This cheap, inexpensive, quick and straightforward method is appropriate for large scale studies. This method could also be applied on paleo-environmental / climatic studies.

Acknowledgments

The authors thank the radiology staff of Jean Verdier hospital (Bondy, Seine Saint Denis, France) for their professional help and patience with computerized x-radiographs and CT scans. We thank Claire E. Lazareth, Henning Kuhnert, Ruth Gingold, Marielle Dumestre, Christine Omuombo, Mercedes Mendez-Millan and two anonymous reviewers for their relevant corrections and comments.

Coral sample R_s was drilled with funds provided by the Vice-rectory of Investigation of the University of Costa Rica (project 808-A8-602) during an internship (N.D.), facilitated by the exchange program of the University of La Rochelle and the University of Costa Rica a program supported by the “Bourse régionale de la découverte” (région Poitou-Charentes). Coral sample R_p was collected during a field trip done in the framework of the HOLBECO project, supported by the French INSU-EC2CO program (managed by the IFREMER Institute).

References

Bosscher, H., 1993. Computerized-Tomography and skeletal density of coral skeletons. Coral Reefs 12, 97–103.

Carricart-Ganivet, J.P., Barnes, D.J., 2007. Densitometry from digitized images of X-radiographs: methodology for measurement of coral skeletal density. Journal of Experimental Marine Biology and Ecology 344, 67–72.

Carricart-Ganivet, J.P., Beltran-Torres, A.U., Merino, M., Ruiz-Zarate, M.A., 2000. Skeletal extension, density and calcification rate of the reef building coral Montastraea annularis (Ellis and Solander) in the Mexican Caribbean. Bulletin of Marine Science 66, 215–224.

Chalker, B.E., Barnes, D.J., Isdale, P., 1985. Calibration of X-ray densitometry for the measurement of coral skeletal density. Coral Reefs 4, 95–100.

Chalker, B.E, Barnes, D.J., 1990. Gamma densitometry for the measurement of skeletal density. Coral Reefs 9, 11–23.

Cooper, T.F., De’Ath, G., Fabricius, K.E., Lough, J.M., 2008. Declining coral calcification in massive Porites in two nearshore regions of the northern Great Barrier Reef. Global Change Biology 14, 529–538.

De’Ath, G., Lough, J.M., Fabricius, K.E., 2009. Declining coral calcification on the Great Barrier Reef. Science 323, 116.

Dustan, P., 1975. Growth and form in reef-building coral Montastrea annularis. Marine Biology 33, 101–107.

Guzman, H.M., Tudhope, A.W., 1998. Seasonal variation in skeletal extension rate and stable isotopic ($^{13}C/^{12}C$ and $^{18}O/^{16}O$) composition in response to several environmental variables in the Caribbean reef coral Siderastrea siderea. Marine Ecology Progress Series. 166, 109–118.

Helmle, K.P., Kohler, K., Dodge, R.E., 2002. Relative optical densitometry and the Coral X-radiograph Densitometry System: Coral XDS. International Society of Reef Studies European Meeting, Cambridge, England.

Helmle, K.P., Dodge, R.E., Ketcham, R.A., 2000. Skeletal architecture and density banding in Diploria strigosa by X-ray computed tomography. Proceedings 9th International Coral Reef Symposium, Bali, Indonesia 23-27 October 2000 1, 365–371.

Hughes, T.P., 1987. Skeletal density and growth form of corals. Marine Ecology Progress Series. 35, 259–266.

IPCC, 2007, R.K., 2007. Climate Change 2007: Synthesis Report. Contribution of working groups I, II and III to the fourth assessment report of the Intergovernmental Panel on Climate Change IPCC.

Kleypas, J.A., 1999. Geochemical consequences of increased atmospheric carbon dioxide on coral reefs. Science 284, 118–120.

Lophaven, S.N., Nielsen, H.B., Søndergaard, J., 2002. A Matlab Kriging Toolbox.
Lough, J.M., Cooper, T.F., 2011. New insights from coral growth band studies in an era of rapid environmental change. Earth Science Reviews
Meredith, W.H., Massey, J.B., 1971. Fundamental physics of radiology. John Wright Sons Ltd, Bristol, 2nd edn 661pp.
Pandolfi, J.M., Connolly, S.R., Marshall, D.J., Cohen, A.L., 2011. Projecting coral reef futures under global warming and ocean acidification. Science 333, 418–422.

Figures

Fig. 1: Computed Radiography (CR) **a** – Scheme of the settings used in this study: the anode-cathode axis is along the x axis, Sp is the x-ray source to IP surface distance, Ss is the x-ray source to coral sample surface and s is the sample thickness **b** – Theoretical irradiation patterns that affects CR, the color scale shows the attenuation of the irradiation; blue: no attenuation, red: high attenuation **c** – Photograph of the two giant clam wedges (d_{clam}) used for the density calibration, scale is given by the one Euro money coin.

Fig. 2: X-radiograph C1 **left:** original and Digitally Detrended image in black and white **right:** Optical Density (OD) variations on the whole image (false colors) and along the red transect (graph). **a** – original image: note the heterogeneities affecting the background, resulting on both effects of inverse square law and heel effect **b** – original background area: saturated margin, sample objects or graphical information have been removed **c** – modeled background **d** – Detrended image: i.e., (b) minus (d).

Fig. 3: Density measured along the reference transects tr_s (**a**) and tr_p (**b**). Black curve is the mean density calculated from the seven corrected images with one standard deviation interval (dark blue). The red curve is the density measured on the CT scan (values are expressed in Hounsfield units). The light blue areas correspond to standard deviation of mean densities calculated from the uncorrected images (1σ). Examples of density transects from uncorrected images are shown (dotted line).

Fig. 4: OD from detrended x-radiograph C2 plotted versus wedge's equivalent thickness (T_{w100}). Red dots: (OD, T_{w100}) pooled dataset. Black line corresponds to a quadratic polynomial fitting. Dashed lines indicate 99% confidence interval.

Fig. 5: Plot of bulk densities (d_{bulk}) of cubes filled with coral powder (squares, n=14) and coral cubes (circles, n=13) versus densities (d_{calc}) calculated from digitally detrended C1.

Tables

Table 1: Characteristics of the computed x-radiographs used in this study

Group	label	Samples orientation*	Sp (cm)	reference samples**	density standard***	kV	mAs	date
A	A1	perpendicular	130	$R_s + R_p$	d_{clam}	73	8.0	04 - 2012
	A2	parallel						
	A3	diagonal						
B	B1	perpendicular	80	$R_s + R_p$	d_{clam}	70	6.4	04 - 2012
	B2	parallel						
	B3	diagonal						
C	C1	perpendicular	100	R_s	d_{powder}	73	8.0	07 - 2010
	C2	perpendicular		R_p + coral cubes	d_{powder} + d_{clam}	73	8.0	11 - 2010

*Along the anode-cathode axis

** R_s: Siderastrea siderea; R_p: Porites sp.

*** d_{clam}: Tridacna squamosa two-sided wedges; d_{powder}: plastic cubes filled with coral powder

Table 2: X-photon energy attenuation for 1 cm air layer and a 30-150 keV energy range (data from: National Institute of Standards and Technology [www.nist.gov]).

x-photon energy (keV)	Energy attenuation for 1 cm air layer (%)
30	0.043
40	0.030
50	0.025
60	0.023
80	0.020
100	0.019
150	0.016

Table 3: Optical Density mean relative difference ΔOD (%) of the x-radiographs background area.

Groups compared	ΔOD range (%)*
intra-group A	8 - 77
intra-group B	15 - 164
intra-group C	59 - 290
A vs. B	25 -147
A vs. C	41 - 223
B vs. C	64 - 198

* Pairs of pixels compared: $9.2 .10^5 < n < 2.3 .10^6$

Table 4: Correlation coefficient R^2 range ($p<0.001$) for transects tr_s and tr_p made on the corrected x-radiographs of groups A, B and C.

Corrected x-radiographs	**tr_s**	**tr_p**
intra-group A	$0.90<R^2<0.98$	$0.99<R^2<1.00$
intra-group B	$0.96<R^2<0.98$	$0.95<R^2<0.99$
inter-groups (A and B)	$0.90<R^2<0.99$	$0.97<R^2<1.00$
all x-radiographs	$0.85<R^2<0.99$	$0.95<R^2<1.00$

Table 5: RSD measured along tr_s and tr_p using the uncorrected and corrected x-radiographs.

	RSD (%) uncorrected	**RSD (%) DD corrected**
intra-group A	10.1	4.8
intra-group B	13.1	4.3
inter-groups (A and B)	16.0	5.5
all x-radiographs	16.1	6.8

Table 6: Correlation coefficient R^2 of transects tr_s made on the corrected x-radiographs versus the measurements made on the CT-scan.

Corrected x-radiographs	**R^2** ($p<0.001$)
A1	0.93
A2	0.96
A3	0.95
B1	0.93
B2	0.94
B3	0.96
C1	0.89

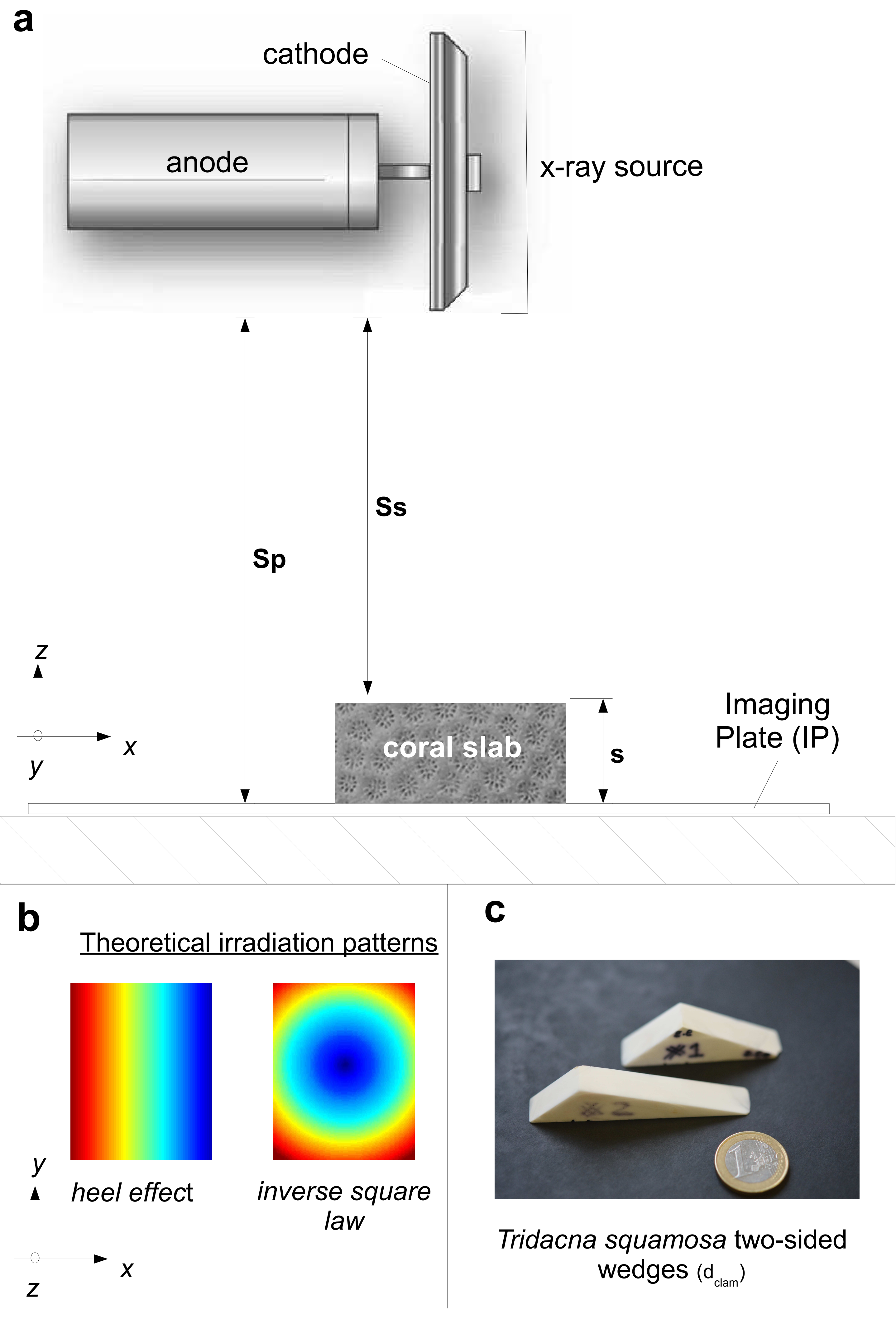

Figure 1_DigCorX-radio

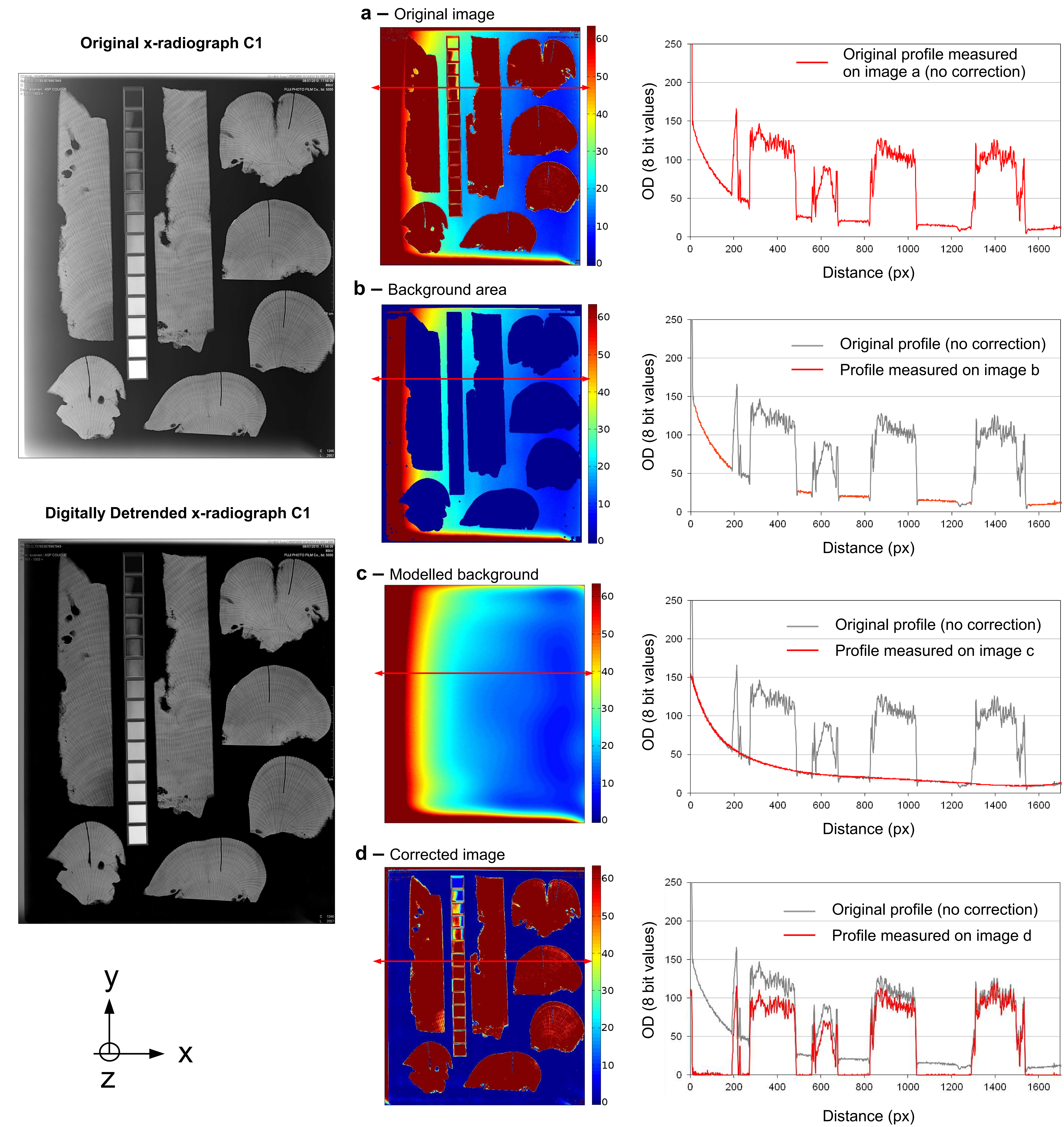

Figure 2_DigCorX-radio

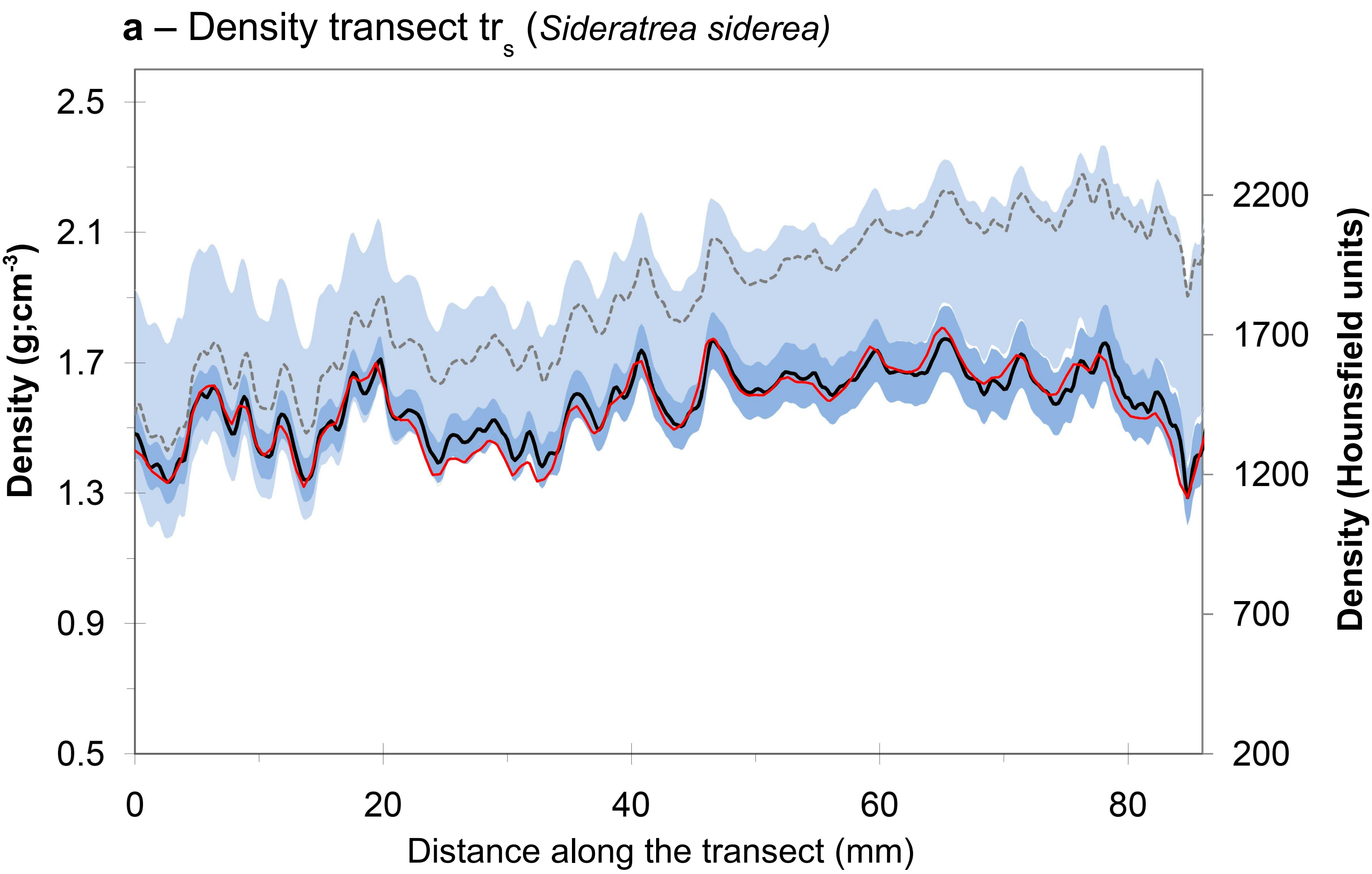

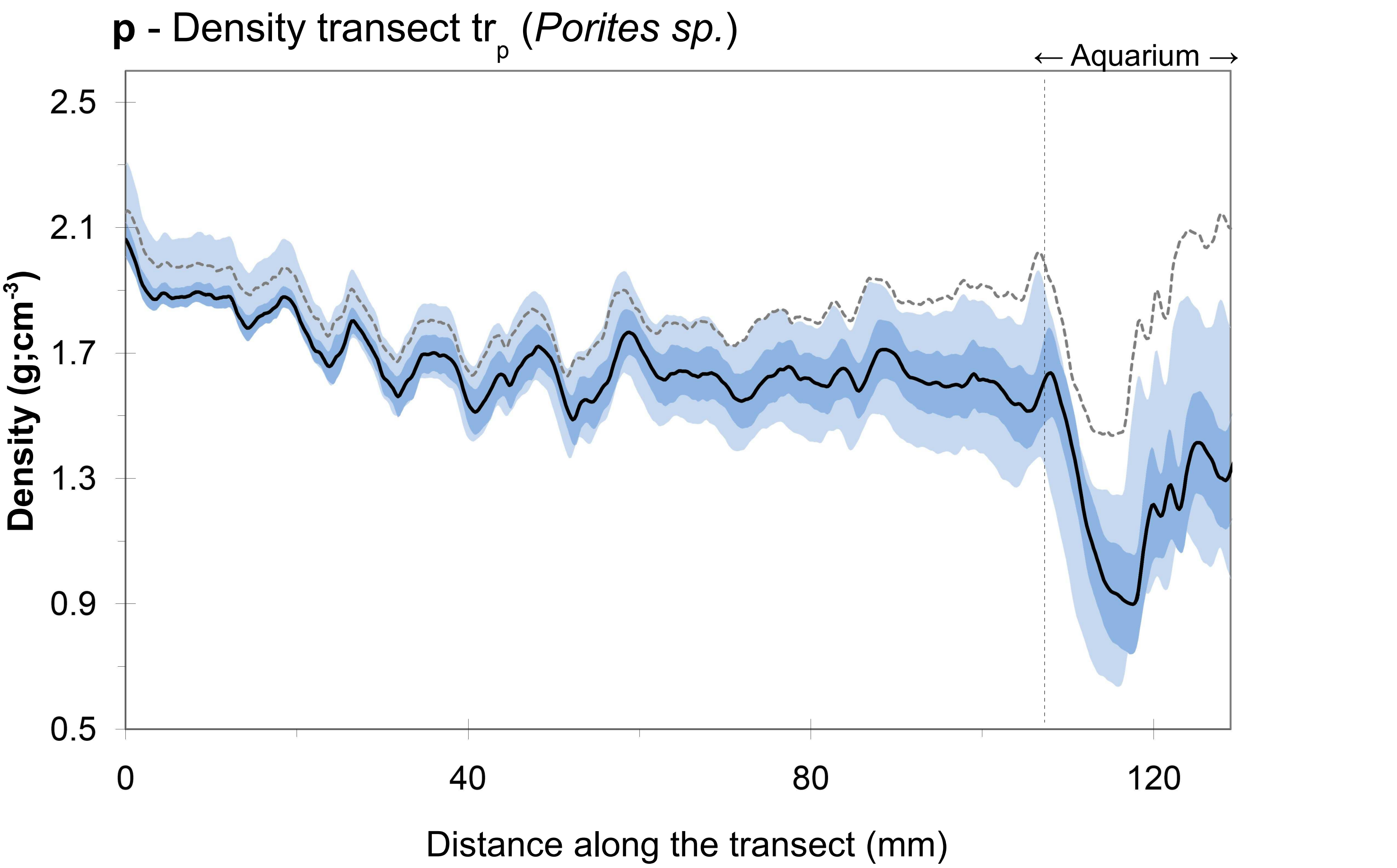

Figure 3 DigCorX-radiographs

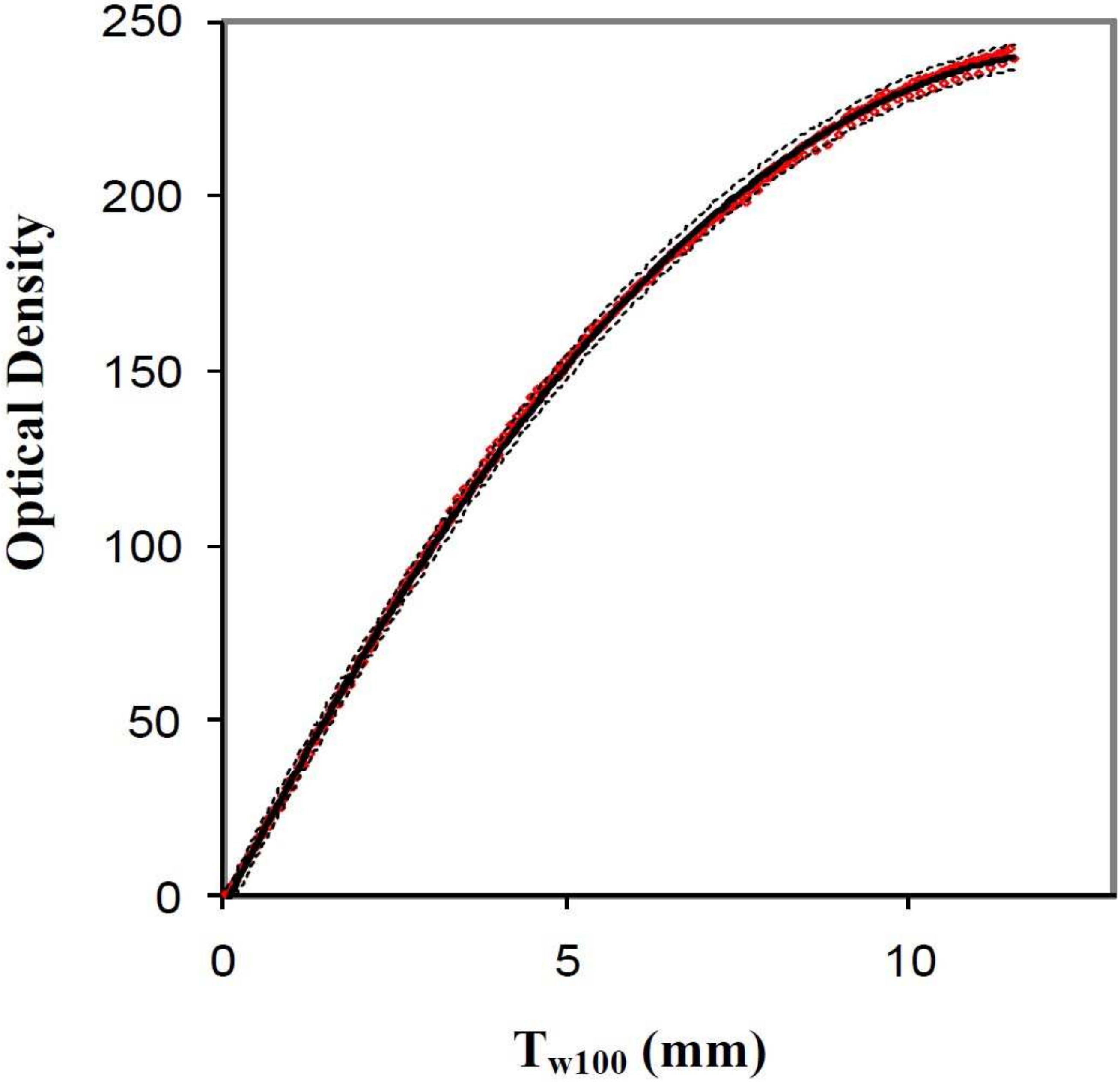

Figure 4_DigCorX-radio

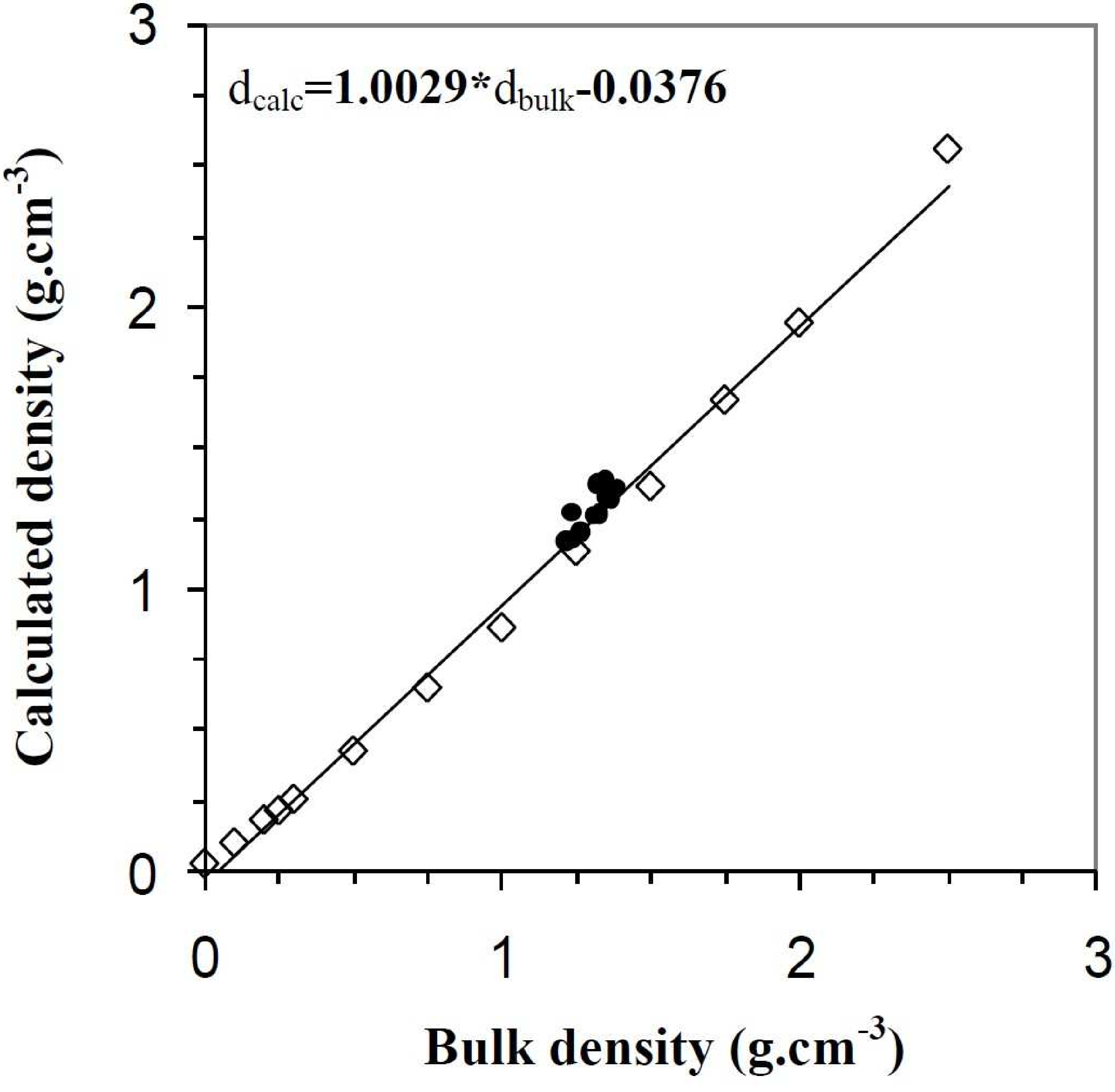

Figure 5_DigCorX-radio